

Interferometric measurement of the biphoton wave function

Federica A. Beduini,^{1,*} Joanna A. Zielńska,¹ Vito G. Lucivero,¹

Yannick A. de Icaza Astiz,¹ and Morgan W. Mitchell^{1,2}

¹*ICFO-Institut de Ciències Fotoniques, Av. Carl Friedrich Gauss, 3, 08860 Castelldefels, Barcelona, Spain*

²*ICREA-Institució Catalana de Recerca i Estudis Avançats, 08015 Barcelona, Spain*

Interference between an unknown two-photon state (a “biphoton”) and the two-photon component of a reference state gives a phase-sensitive arrival-time distribution containing full information about the biphoton temporal wave function. Using a coherent state as a reference, we observe this interference and reconstruct the wave function of single-mode biphotons from a low-intensity narrowband squeezed vacuum state.

Introduction - Correlated photon pairs, or “biphotons,” are a paradigmatic experimental system in quantum technology, with applications in quantum communications [1], quantum information processing [2], foundations of physics [3] and quantum metrology [4]. In many experiments, the performance of a biphoton source is closely tied to the two-photon wave function (TPWF) that describes the temporal correlations of the photons. For example, the visibility of Hong-Ou-Mandel interference depends on the TPWF, even when some other degree of freedom, e.g. polarization, is used to encode quantum information [5]. Measurements of the TPWF are also used to characterize realistic photon pairs sources, allowing the diagnosis of experimental defects, e.g. imperfect poling in the down-conversion crystal [6] or dispersion [7].

The TPWF $\psi(t_1, t_2)$ is an intrinsically multi-dimensional object, depending on the two time coordinates t_1 and t_2 [8]. Methods to characterize the TPWF include measurement of the joint spectral density [9], measurement of the joint temporal density [6], non-classical interference using the Hong-Ou-Mandel effect [10–12], and nonlinear optical processes [7, 13–15]. All of these techniques give partial information about the TPWF. For example, the joint temporal density gives the magnitude $|\psi(t_1, t_2)|$, while the joint spectral density gives the magnitude of Fourier components.

Full measurement of the TPWF requires a phase-sensitive and tomographic measurement, applied to a continuous range of time values. Some elements of this approach have been demonstrated: Quantum state tomography [16] has been widely used to characterize aggregate measures of a quantum state, e.g. the integrated field of a pulse, or the mode describing a single frequency component. This includes traditional homodyne methods using strong local oscillators [16] and mesoscopic methods using weak local oscillators plus photon-counting detection [17]. Homodyne characterization of a single photon wave function has also been reported [18, 19].

Here we demonstrate full characterization of a two-photon wave function, based on the phenomenon of in-

terference of two-photon amplitudes [20, 21]. A similar method is proposed in [22]. Our approach combines the use of a weak phase reference and photon counting detection as in [17] with wave-function detection over an extended time-span as in [18, 19], and adds the new elements of time-correlated photon counting, as required by the dimensionality of the TPWF. We demonstrate the method by reconstructing the TPWF of single-mode squeezed vacuum from a sub-threshold OPO. An attractive feature of our approach is a very direct data interpretation, without the ill-posed inverse problem typically encountered in tomography.

One- and two-photon wavefunctions - We use field correlations functions [23] to characterize optical quantum states. For a state $|\lambda\rangle$, the so-called “one-photon wave function” is $\psi_i^{(\lambda)}(t) \equiv \langle 0|E_i^{(+)}(t)|\lambda\rangle$, where $E_i^{(+)}(t)$ is the positive-frequency part of the electric field operator for mode i . Because $E_i^{(+)}(t)$ removes one photon, this represents $|\lambda\rangle$ projected onto the one-photon subspace. Similarly, the “two-photon wave function” is [10]

$$\psi_{i,j}^{(\lambda)}(t_1, t_2) \equiv \langle 0|E_i^{(+)}(t_1)E_j^{(+)}(t_2)|\lambda\rangle. \quad (1)$$

As with Schrödinger wave functions, neither $\psi_i^{(\lambda)}(t)$ nor $\psi_{i,j}^{(\lambda)}(t_1, t_2)$ is directly observable. On the other hand, the second-order intensity correlation function

$$g_{ij}^{(2)}(t_1, t_2) \propto \langle \lambda|E_j^{(-)}(t_2)E_i^{(-)}(t_1)E_i^{(+)}(t_1)E_j^{(+)}(t_2)|\lambda\rangle \quad (2)$$

is directly observable in photon pair arrival time distributions. In the commonly-encountered case that $|\lambda\rangle$ contains no more than two photons, this is proportional to $|\psi_{ij}^{(\lambda)}(t_1, t_2)|^2$. The second order correlation function then gives important but incomplete information about the two-photon wavefunction, as it contains no information on the phase of $\psi_{ij}^{(\lambda)}$, which is a complex function.

Coherent state reference - We consider a scenario in which $|\lambda\rangle$ occupies one propagating mode (V), while a time-independent coherent state $|\alpha\rangle$ occupies an ancilla mode (H). We measure the correlation function

$$\tilde{\psi}_{AB}^{(\kappa)}(t_1, t_2) = \langle 0|\tilde{E}_A^{(+)}(t_1)\tilde{E}_B^{(+)}(t_2)|\kappa\rangle \quad (3)$$

* federica.beduini@icfo.es

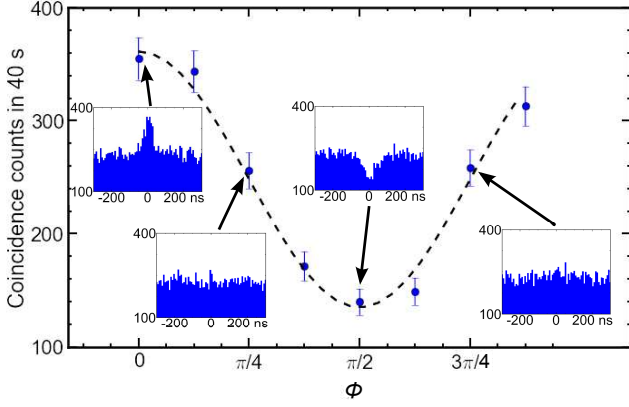


FIG. 2. (Color online). Arrival-time distributions showing interference of two-photon amplitudes. Main graph shows coincidence rates $g_{AB(\kappa)}^{(2)}(0)$ (circles) for delay $\tau = 0$ versus analysis phase ϕ . These show a sinusoidal behaviour (dashed line, $A + B \cos 2\phi$ fit to the data) revealing two-photon interference as predicted by (7). Insets show $g_{AB(\kappa)}^{(2)}(\tau)$ for the values of ϕ indicated with arrows. These clearly show the passage from constructive interference at $\phi = 0$, where a peak is visible, to destructive interference at $\phi = \pi/2$, where a dip appears. Error bars show $\pm 1\sigma$ (standard deviation) statistical uncertainty.

beams by a calcite beam displacer and passed through a narrowband (445 MHz) atomic filter [25, 26], in order to isolate the squeezed vacuum and block with high efficiency the hundreds of non-degenerate frequency modes generated by the OPO. The maximum transmission frequency of this filter is located at 2.7 GHz to the red of the center of the rubidium D_1 line, and the laser frequency is stabilised at this particular frequency by using an integrated electro-optic modulator to add sidebands to the laser prior to the saturated absorption spectroscopy. Each filtered beam is then coupled into a single-mode fiber and split with a 50/50 fiber beam splitter to a pair of single-photon counting avalanche photo diodes. A time-of-flight recorder time-stamps each arrival and correlations are computed on a PC.

A low OPO pump power (1 mW, 0.04% of threshold) is used so that contributions of more than two photons are negligible. The coherent reference power is chosen to give a similar rate of two-photon events, for high visibility interference, as seen in Fig. 2. The relative phase ϕ_{rel} between the coherent and the squeezed beam is stabilized by a quantum noise lock: One Stokes component is detected with a balanced polarimeter, and the noise power in a 3 Hz bandwidth above 500 kHz is computed analogically using a multiplier circuit. This signal is fed back by a servo loop to a piezo-electric actuator on a mirror in the pump path, to stabilize the pump phase by a side-of-fringe lock. A galvanometer mirror is used to switch between the single-photon counting and stabilisation setups at a frequency of ~ 100 Hz. The reference beam power is increased during the stabilization part of

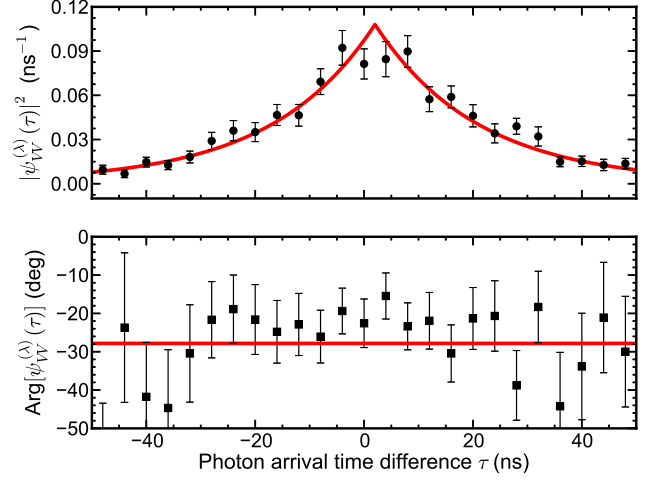


FIG. 3. (Color online). Squared amplitude (above) and phase (below) of the reconstructed two-photon wave function for the squeezed vacuum state. The solid line shows the predicted, double exponential amplitude describing an ideal squeezed vacuum state from our OPO with an independently-measured 8.1 MHz bandwidth. The amplitude and the horizontal offset were fit to the data. Error bars show $\pm 1\sigma$ statistical uncertainty assuming Poisson statistics and using propagation of error through Eqs. (8) and (9).

the cycle, to reach the shot-noise-limited regime optimal for detection of the squeezing and operation of the noise lock. Two cascaded AOMs, whose RF power is chopped synchronously with the galvanometer mirror, modulate the coherent reference beam power, so that it has high power when the light is entering the stabilisation setup and low power when the photon counting part is active. The system can maintain a fixed ϕ_{rel} over several hours. **Results** - As our light source is continuous-wave, the light statistics are stationary: the correlations and wave function depend only on the photon arrival-time difference $\tau = t_1 - t_2$. We compute the experimental $g_{AB(\kappa)}^{(2)}(\tau)$ from coincidences between detector groups A and B in Fig. 1, with a 4 ns coincidence window, a compromise between temporal resolution and statistical significance.

As shown in Fig. 2, we observe both constructive and destructive interference, e.g. at $\phi = 0$ and $\phi = \pi/2$, respectively. The observation of a dip in the correlation function is especially interesting, because it clearly signals destructive interference of two-photon amplitudes from the coherent and the squeezed vacuum states. The interference visibility is limited by accidental coincidence counts, which are mainly due to the residual OPO locking beam and to non-degenerate modes passing through the filter [26]. However, these do not affect the wavefunction reconstruction: the accidentals add a term independent from τ to the $g^{(2)}$, which is canceled by the subtractions in Eq. (8).

We next collect $g_{AB(\kappa)}^{(2)}(\tau)$ data for $\phi = 0, \pi/3, 2\pi/3$ and use Eqs. (8) and (9) to reconstruct $\psi_V^{(\lambda)}(\tau)$, shown in

Fig. 3. The reconstruction is direct: $\psi_{VV}^{(\lambda)}$ at a given τ depends only on coincidence events at that value of τ . The results are consistent with a double-exponential amplitude with 26 ns full-width at half-maximum (FWHM), as expected for a squeezed vacuum state from an OPO with the 8.1 MHz FWHM bandwidth independently-measured on our system. Fig. 3 also shows a constant but nonzero phase of the wave function. A constant phase is expected for an ideal OPO, while a phase defect could signal cavity or crystal imperfections [6, 7]. The phase offset is tunable via the side-of-fringe lock that sets the relative phase of the squeezed vacuum and reference, and is another indication of interference at the two-photon level.

Conclusion - We have demonstrated complete measurement of the complex temporal wave function of biphotons using interference of the two-photon amplitude against a reference. The interference gives a phase-sensitive arrival-time distribution, from which we reconstruct the biphoton wave function. In contrast to most tomographic procedures [5, 16], only three measurement settings are required to find the real and imaginary parts of the wave function, as well as the strength of the ref-

erence state. The inverse problem is thus neither overdetermined nor under-determined, and can be solved analytically. We analyze the output of a narrow-band, atom-resonant OPO operating at 795 nm, and find a biphoton wave-function consistent with squeezed-vacuum biphotons from an ideal OPO with our measured line-width.

The technique shows clearly the interference of two-photon amplitudes from distinct sources, and may be useful for detecting and correcting errors in quantum light sources for quantum information processing [27], quantum communications [28], and quantum metrology [29].

Acknowledgements - We thank F. Wolfgramm and F. Martin Ciurana for helpful discussions. This work was supported by the Spanish MINECO project MAGO (Ref. FIS2011-23520), European Research Council project AQUMET and by Fundació Privada CELLEX. J.Z. was supported by the FI-DGR PhD-fellowship program of the Generalitat of Catalonia. Y. A. de I. A. was supported by the scholarship BES-2009-017461, under project FIS2007-60179.

-
- [1] C.-Z. Peng, T. Yang, X.-H. Bao, J. Zhang, X.-M. Jin, F.-Y. Feng, B. Yang, J. Yang, J. Yin, Q. Zhang, N. Li, B.-L. Tian, and J.-W. Pan, *Phys. Rev. Lett.* **94**, 150501 (2005).
 - [2] P. Walther, K. J. Resch, T. Rudolph, E. Schenck, H. Weinfurter, V. Vedral, M. Aspelmeyer, and A. Zeilinger, *Nature* **434**, 169 (2005).
 - [3] M. Giustina, A. Mech, S. Ramelow, B. Wittmann, J. Kofler, J. Beyer, A. Lita, B. Calkins, T. Gerrits, S. W. Nam, R. Ursin, and A. Zeilinger, *Nature* **497**, 227 (2013).
 - [4] M. W. Mitchell, J. S. Lundeen, and A. M. Steinberg, *Nature* **429**, 161 (2004).
 - [5] R. B. A. Adamson, L. K. Shalm, M. W. Mitchell, and A. M. Steinberg, *Phys. Rev. Lett.* **98**, 043601 (2007).
 - [6] O. Kuzucu, F. N. C. Wong, S. Kurimura, and S. Tovstonog, *Phys. Rev. Lett.* **101**, 153602 (2008).
 - [7] K. A. O'Donnell and A. B. U'Ren, *Phys. Rev. Lett.* **103**, 123602 (2009).
 - [8] A. Valencia, A. Ceré, X. Shi, G. Molina-Terriza, and J. P. Torres, *Phys. Rev. Lett.* **99**, 243601 (2007).
 - [9] P. J. Mosley, J. S. Lundeen, B. J. Smith, P. Wasylczyk, A. B. U'Ren, C. Silberhorn, and I. A. Walmsley, *Phys. Rev. Lett.* **100**, 133601 (2008).
 - [10] A. Sergienko, Y. Shih, and M. Rubin, *JOSA B* **12**, 859 (1995).
 - [11] V. Giovannetti, L. Maccone, J. H. Shapiro, and F. N. C. Wong, *Phys. Rev. A* **66**, 043813 (2002).
 - [12] R. Okamoto, S. Takeuchi, and K. Sasaki, *Phys. Rev. A* **74**, 011801 (2006).
 - [13] B. Dayan, A. Pe'er, A. A. Friesem, and Y. Silberberg, *Phys. Rev. Lett.* **93**, 023005 (2004).
 - [14] A. Pe'er, B. Dayan, A. A. Friesem, and Y. Silberberg, *Phys. Rev. Lett.* **94**, 073601 (2005).
 - [15] S. Sensarn, I. Ali-Khan, G. Y. Yin, and S. E. Harris, *Phys. Rev. Lett.* **102**, 053602 (2009).
 - [16] D. T. Smithey, M. Beck, M. G. Raymer, and A. Faridani, *Phys. Rev. Lett.* **70**, 1244 (1993).
 - [17] G. Puentes, J. S. Lundeen, M. P. A. Branderhorst, H. B. Coldenstrodt-Ronge, B. J. Smith, and I. A. Walmsley, *Phys. Rev. Lett.* **102**, 080404 (2009).
 - [18] J. S. Neergaard-Nielsen, B. M. Nielsen, C. Hettich, K. Mølmer, and E. S. Polzik, *Phys. Rev. Lett.* **97**, 083604 (2006).
 - [19] O. Morin, C. Fabre, and J. Laurat, *Phys. Rev. Lett.* **111**, 213602 (2013).
 - [20] J. R. Torgerson and L. Mandel, *J. Opt. Soc. Am. B* **14**, 2417 (1997).
 - [21] Y. J. Lu and Z. Y. Ou, *Phys. Rev. Lett.* **88**, 023601 (2001).
 - [22] C. Ren and H. F. Hofmann, *Phys. Rev. A* **86**, 043823 (2012).
 - [23] R. J. Glauber, *Phys. Rev.* **130**, 2529 (1963).
 - [24] A. Predojević, Z. Zhai, J. M. Caballero, and M. W. Mitchell, *Phys. Rev. A* **78**, 063820 (2008).
 - [25] J. A. Zielińska, F. A. Beduini, N. Godbout, and M. W. Mitchell, *Optics letters* **37**, 524 (2012).
 - [26] J. A. Zielińska, F. A. Beduini, V. G. Lucivero, and M. W. Mitchell, *ArXiv e-prints* (2014), arXiv:1406.3968 [quant-ph].
 - [27] F. Wolfgramm, X. Xing, A. Ceré, A. Predojević, A. M. Steinberg, and M. W. Mitchell, *Opt. Express* **16**, 18145 (2008).
 - [28] J. Fekete, D. Rieländer, M. Cristiani, and H. de Riedmatten, *Phys. Rev. Lett.* **110**, 220502 (2013).
 - [29] F. Wolfgramm, C. Vitelli, F. A. Beduini, N. Godbout, and M. W. Mitchell, *Nat Photon* **7**, 28 (2013).